



Technical Note

# QDA-System: A Cloud-Based System for Monitoring Water Quality in Brazilian Hydroelectric Reservoirs from Space

Marcelo Curtarelli \*, Edmar Neto, Fanny de Siqueira, Felipe Yopan, Gilmar Soares, Gilnei Pauli , João de Souza, Luana Silva, Marcio Sagaz, Miguel Demay, Natália Bortolas, Ricardo Yoshimura and Vitor Guimarães

Fundação CERTI, Florianópolis 88040-970, Brazil; ept@certi.org.br (E.N.); fcs@certi.org.br (F.d.S.); fsy@certi.org.br (F.Y.); ggs@certi.org.br (G.S.); gui@certi.org.br (G.P.); jhb@certi.org.br (J.d.S.); ldv@certi.org.br (L.S.); msg@certi.org.br (M.S.); mbd@certi.org.br (M.D.); nob@certi.org.br (N.B.); rsy@certi.org.br (R.Y.); vs@certi.org.br (V.G.)

\* Correspondence: mei@certi.org.br

**Abstract:** This article presents the QDA-System (*Sistema Qualidade da Água*, from Portuguese), a system developed to monitor the quality of surface waters in Brazilian hydroelectric reservoirs using satellite images and cloud computing services. The development requirements of the QDA-System considered its use for operational monitoring purposes, with all processing steps automated, and a user-friendly interface to access and query the data generated automatically by the system. A pilot application of the QDA-System was customized and implemented for monitoring the Foz do Chapecó hydroelectric reservoir located in southern Brazil. For the pilot application, the QDA-System was customized to estimate nine water quality parameters; five were estimated directly from Sentinel-2 multispectral images and four were estimated indirectly. We expect that in the near future the QDA-System can be replicated to monitor other Brazilian reservoirs, bringing benefits and cost reduction related to water quality monitoring, not only for the sector of hydroelectric generation but for other sectors that also need similar monitoring, such as sanitation and aquaculture production.



**Citation:** Curtarelli, M.; Neto, E.; de Siqueira, F.; Yopan, F.; Soares, G.; Pauli, G.; de Souza, J.; Silva, L.; Sagaz, M.; Demay, M.; et al. QDA-System: A Cloud-Based System for Monitoring Water Quality in Brazilian Hydroelectric Reservoirs from Space. *Remote Sens.* **2022**, *14*, 1541. <https://doi.org/10.3390/rs14071541>

Academic Editor: Teodosio Lacava

Received: 23 February 2022

Accepted: 22 March 2022

Published: 23 March 2022

**Publisher's Note:** MDPI stays neutral with regard to jurisdictional claims in published maps and institutional affiliations.



**Copyright:** © 2022 by the authors. Licensee MDPI, Basel, Switzerland. This article is an open access article distributed under the terms and conditions of the Creative Commons Attribution (CC BY) license (<https://creativecommons.org/licenses/by/4.0/>).

**Keywords:** cloud computing; satellite images; bio-optical modeling; reservoirs; lakes

## 1. Introduction

The use of remote sensing images for the study of inland water bodies dates back to the 1970s, initially focusing on the development of local models with temporally limited studies [1]. Over the last 50 years, the development of information and image collection technologies has allowed great advances in the field of remote sensing of water, such as the study of multiple parameters [2], the development and the improvement of different approaches for bio-optical modeling [3], the expansion of the temporal and spatial scales of analysis [1], and born of monitoring initiatives such as Satellite earth observations for lake monitoring (OLakeWatch) [4] in Canada and the Cyanobacteria Assessment Network (CyAN) in the USA [5]. All of these advances in terms of basic and applied research have paved the way for us to move forward in the innovation chain through the pilot development of an automatic system for monitoring water quality parameters from space.

Recently, some solutions were developed that combine the use of remote sensing data and cloud computing for the monitoring and the forecasting of different environmental issues. As examples of solutions presented in the literature, we can mention a cloud-based flood warning system [6], a cloud-based system to monitor land use and land cover [7], and an algal bloom alert system [8]. The main advantages of this approach are the use of cloud computing power to process large amounts of data and the absence of a need to download the data to a local server.

Taking into account the need to modernize and to expand the monitoring capacity of Brazilian hydroelectric reservoirs, the CERTI Foundation conducted the Research and

Development (R&D) project “00642-2705/2019-Development of a system for remote monitoring of water quality in water reservoirs based on multispectral images,” financed by the Brazilian Electric Energy Agency (ANEEL), with the main objective of developing a system based on cloud computing technology for monitoring inland water bodies. This article aims to present the developed system and its pilot application for monitoring the surface water of the Foz do Chapecó hydroelectric plant reservoir in southern Brazil.

## 2. QDA-System Design and Development

The monitoring system (hereafter called the QDA-System) was designed using state of the art cloud computing and remote sensing techniques applied to inland water monitoring and bio-optical modeling [3]. The QDA-System was developed to routinely monitor surface water quality in lakes and reservoirs using satellite images and auxiliary data (e.g., residence time, bathymetry, and in situ parameters), allowing the emission of alerts considering rules and thresholds predefined by users. The system was developed in the Python programming language using different computing and cloud storage services offered by Amazon Web Services (AWS), but it can also be deployed and run in other commercial clouds (e.g., Google Cloud or Microsoft® Azure Cloud). For its development, the following requirements were considered:

1. Operational monitoring: A systematic and routine provision of information of various water quality parameters;
2. Automated processing: Achieved without the need for interactions or processing performed by system operators;
3. Customizable: The capacity to use multiple image sources (e.g., Sentinel-2 MSI, Landsat-8 OLI, Planet®) and implementation of different types of water quality models according to site-specific needs;
4. Scalable: The capacity to be easily replicated and parameterized for different water bodies;
5. User-friendly interface with different access levels: developed for accessing via an intuitive web interface, with different access levels, considering specific needs.

### *Digital Image Processing, Bio-Optical Modeling, and Water Quality Index Computation*

The main digital image processing tasks implemented in the pilot version of the QDA-System includes: (1) mosaic images of different tiles (if necessary); (2) resample band images to the same pixel size; (3) the application of scale factors to convert digital number to surface reflectance value; (4) applying a water mask over the target area; and (5) creating and applying a cloud or shadow mask.

The QDA-System supports the implementation of empirical and semi-empirical bio-optical models to estimate optically active and inactive parameters [2,3]. The optically active parameters are those related to the Optically Active Constituents (OAC) that are responsible for the absorption and scattering of electromagnetic energy in the water column and directly related to the satellite measurements. On the other hand, the optically inactive parameters do not interfere in the underwater light field; consequently, they cannot be directly related to measurements taken by satellites. Even so, they can be obtained indirectly from relationships with optically active parameters [2].

The QDA-System also supports the computation of water quality indexes based on estimated parameters combined with in situ measurements that can be entered into the system using spreadsheets. Figure 1 shows the workflow of processing tasks and water quality parameters developed for the first version of the QDA-System based on the use of MSI Sentinel-2 images (detailed in Section 3.2.2).

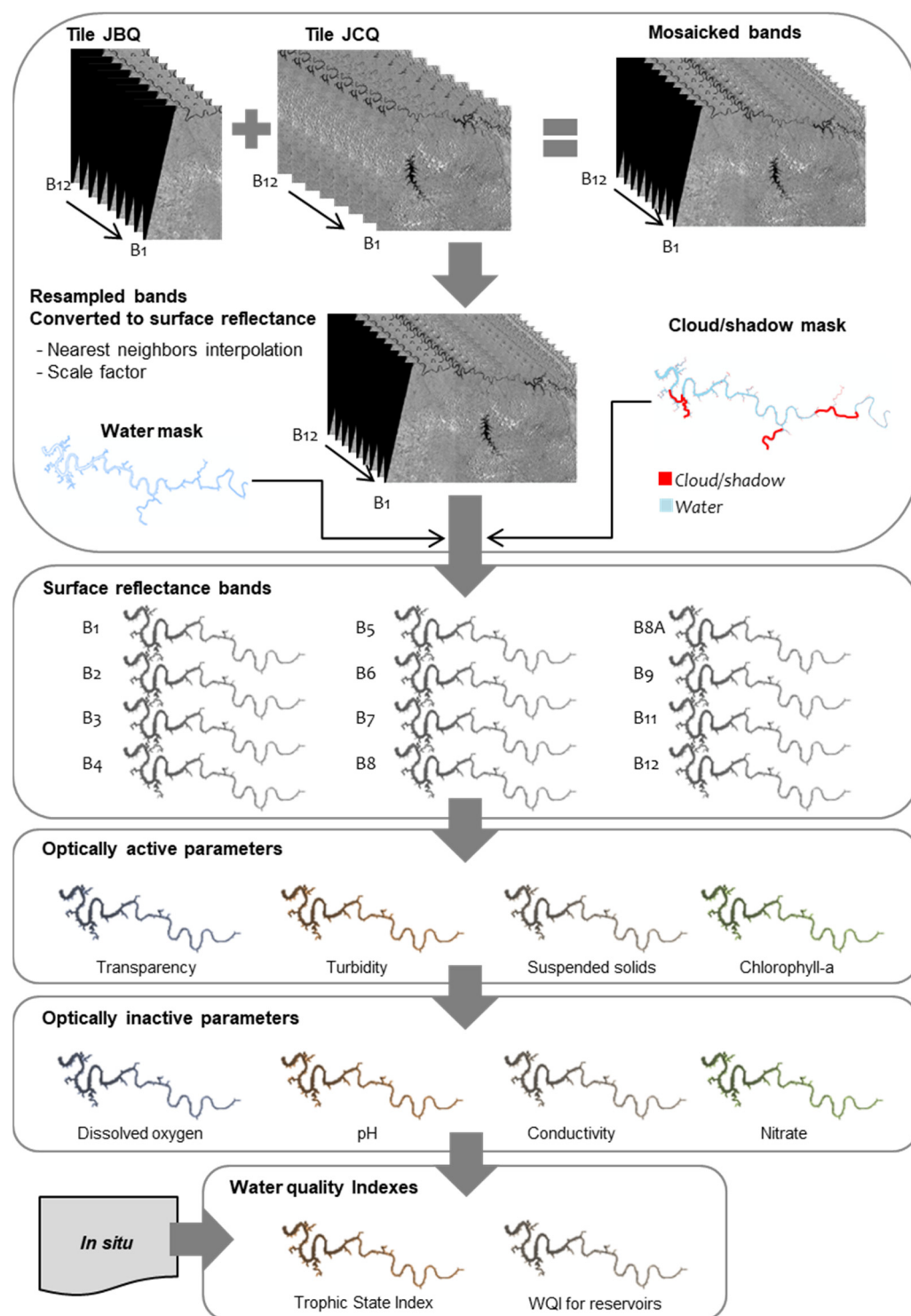


**Figure 1.** Workflow of processing tasks and water quality parameter retrieval implemented in the QDA-System: example from pilot case. B1 to B12 refers to Sentinel-2 MSI multispectral bands.

### 3. Study Case—Foz do Chapecó Reservoir

#### 3.1. Site Description

A pilot version of the QDA-System was implemented to monitor the surface water quality of the Foz do Chapecó Hydroelectric Reservoir (FCHR) located in southern Brazil near the city of Chapecó (Figure 2). The FCHR has a latitudinal elongated shape with 79 km<sup>2</sup> of surface area and a mean depth of 18.8 m, covering the area of 12 municipalities [9].

Besides energy production, the FCHR has other uses, such as domestic water supply, irrigation, recreation, fishing, and navigation [10].

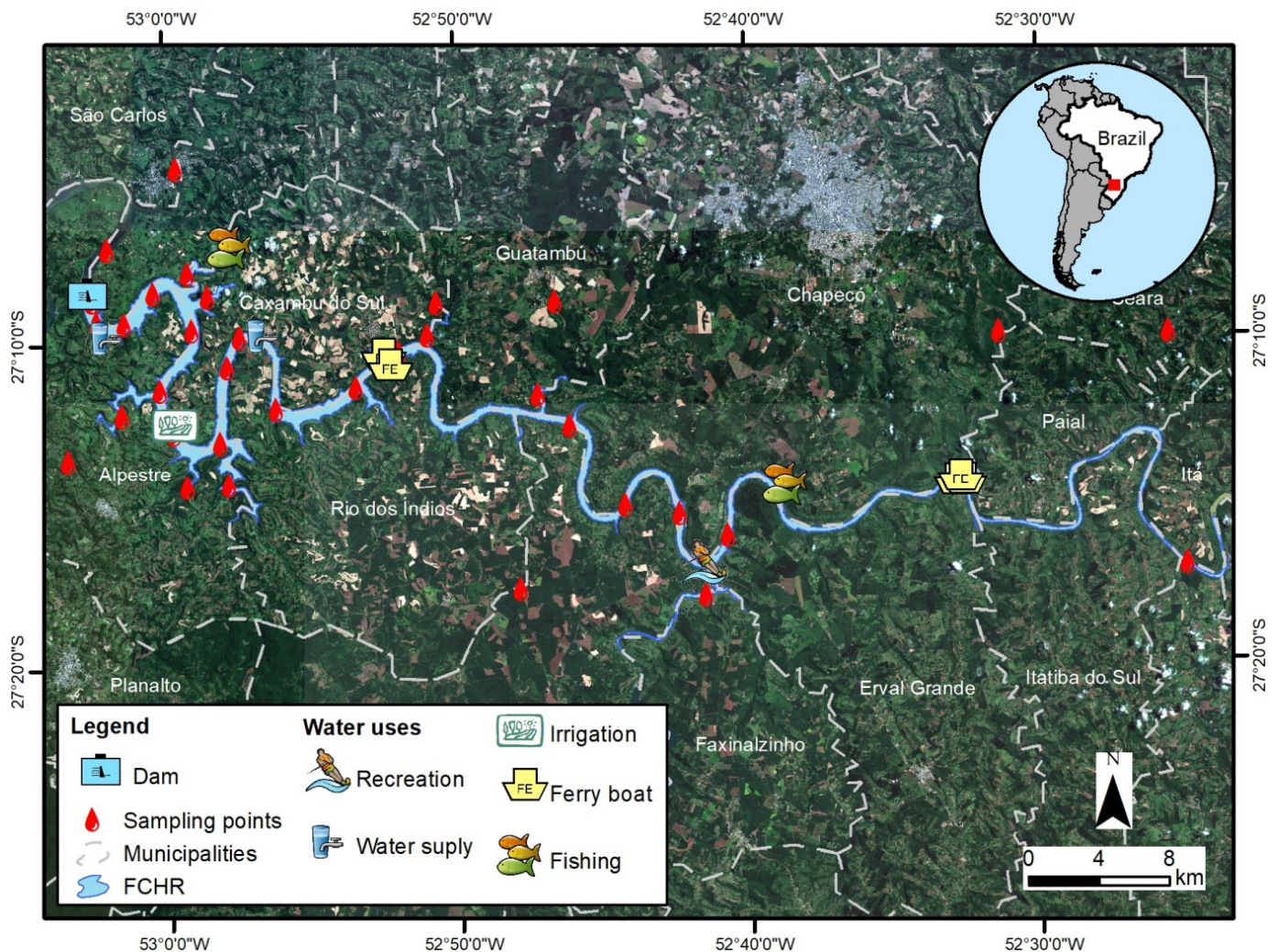


**Figure 2.** Pilot area location and settings.

### 3.2. Selected Parameters and Available Dataset

For the pilot application, a set of nine water quality parameters were previously selected, five of which were obtained directly from satellite images (optically active) and four that were obtained indirectly (optically inactive):

1. Optically active: (1) Chlorophyll-*a* (Chl-*a*); (2) Floating macrophytes; (3) Total of Suspended Solids (TSS); (4) Turbidity; and (5) Water transparency (Secchi Disk Depth—SDD);
2. Optically inactive: (1) Conductivity; (2) Dissolved oxygen (DO); (3) Nitrate; and (4) pH.

The dataset available for model calibration and validation included 178 water samples collected during 11 campaigns (see locations in Figure 1), distributed between February 2019 and May 2021, covering all phases of the hydrological cycle and the different operational conditions of the FCHR (Table 1). All campaigns had concurrent passages of Sentinel-2 satellites.

**Table 1.** Summary of calibration and validation dataset available for FCHR.

| Field Campaign | Data             | Image Acquisition                        | Sampling Points |
|----------------|------------------|--|-----------------|
| 1              | 22 February 2019 | 22 February 2019                         | 14              |
| 2              | 18 April 2019    | 18 April 2019                            | 14              |
| 3              | 8 August 2019    | 6 August 2019                            | 14              |
| 4              | 11 October 2019  | 10 October 2019                          | 17              |
| 5              | 20 December 2019 | 19 December 2019                         | 17              |
| 6              | 12 February 2020 | 12 February 2020                         | 18              |
| 7              | 12 February 2020 | 10 February 2020 and<br>12 February 2020 | 17              |
| 8              | 27 May 2020      | 25 May 2020 and 27 May 2020              | 18              |
| 9              | 23 November 2020 | 23 November 2020                         | 18              |
| 10             | 10 December 2020 | 8 December 2020                          | 13              |
| 11             | 27 May 2021      | 27 May 2021                              | 18              |

### 3.2.1. In Situ Data

The water sample collections were conducted by *Aquaeris Engenharia e Soluções Ambientais* LTDA, a third-party company specializing in this type of service. All the field surveys followed the specification and the protocols presented in the Brazilian guide for collection and preservation of samples [11]. Conductivity, dissolved oxygen, pH, and turbidity were measured using a multiparameter probe (Akso [www.akso.com.br](http://www.akso.com.br) (accessed on 4 January 2022), model AK88). The water transparency was measured using a Secchi disk. The remaining parameters were analyzed in the laboratory following the Standard Methods for the Examination of Water and Wastewater (SMEWW) [12] and U.S. Environmental Protection Agency [13] procedures.

### 3.2.2. Satellite Images

The Sentinel-2 mission was chosen for the pilot application [14]. The mission consisted of two satellites, Sentinel-2A and Sentinel-2B, both carrying the Multispectral Instrument (MSI). The joint use of the 2 satellites allowed the acquisition of 73 images of the complete reservoir throughout the year (1 image every 5 days), with spatial resolution ranging from 10 to 60 m depending on the spectral band. The product chosen for the application was the level 2A satellite which provided systematic surface reflectance ortho-images (more information about the 2A algorithm is available at: <https://earth.esa.int/web/sentinel/technical-guides/sentinel-2-msi/level-2a/algorithm> (accessed on 4 January 2022)).

For this pilot application, the QDA-System was configured to access the Copernicus Open Access Hub (<https://scihub.copernicus.eu/> (accessed on 3 January 2022)) using the application programming interface (API) and to download the images to be processed by the QDA-System.

### 3.3. Model Calibration and Validation

For each modeled water quality parameter, the available dataset was analyzed individually in order to remove samples with values lower than the limit of quantification and detection, outliers and samples located in pixels covered by cloud or shadows, or with low quality. The sample points considered valid for a given parameter were split into two subsets: one was used for model calibration (between 60 and 70% of valid points) and the other was used for model validation (between 30 and 40% of valid points).

The model calibration was performed through adjustments using an ordinary least squares regression method. For the optically active parameter (except for floating macrophytes), we tested different univariate models (empirical and semi-empirical) and different types of adjustments (linear, polynomial, exponential, and power), resulting in more than

1200 regression analyses. For the optically inactive parameters, we tested empirical univariate models relating them to the optically active parameters, resulting in more than 1000 regression analyses. The criteria used to select the best calibrated model for each parameter were the  $p$ -value and the coefficient of determination ( $R^2$ ).

The model validation was conducted using the validation subset and the metrics presented by [15] that compare the values estimated by the calibrated models to the in situ measurements:

$$R^2 = 1 - \left( \frac{SS_{\text{res}}}{SS_{\text{tot}}} \right)$$

where  $SS_{\text{res}}$  is the residual sum of squares and  $SS_{\text{tot}}$  is the total sum of squares.

$$\text{MAD} = \frac{\sum_{i=1}^n |y_i - \bar{y}_i|}{n}$$

where MAD is the mean absolute deviation,  $y_i$  is the observed value,  $\bar{y}_i$  is the predicted value, and  $n$  is the sample size.

$$\text{MSE} = \frac{\sum_{i=1}^n (y_i - \bar{y}_i)^2}{n}$$

where MSE is the mean squared error.

$$\text{RMSE} = \sqrt{\frac{\sum_{i=1}^n (y_i - \bar{y}_i)^2}{n}}$$

where RMSE is the root mean squared error.

$$\text{MAPE} = \frac{\sum_{i=1}^n \left| \frac{y_i - \bar{y}_i}{y_i} \right|}{n} \times 100$$

where MAPE is the mean absolute percentage error (%).

After the validation procedure, the model with best performance for each parameter was configured in the QDA-System.

### Floating Macrophytes

The automatic detection of floating macrophytes is performed by applying thresholds and histogram slicing on a Vegetation Index (VI), which is widely used in the literature. For the pilot application, 4 VI were tested: (1) the Normalized Difference Vegetation Index (NDVI) [16], (2) the Enhanced Vegetation Index (EVI) [17], (3) the Normalized Difference Aquatic Vegetation Index (NDAVI) [18] and (4) the Water Adjusted Vegetation Index (WAVI) [19]. The best VI and threshold to detect floating macrophytes was defined empirically, by comparing values extracted from seven selected images where floating macrophytes were clearly visible. The performance of the VIs and thresholds used to detect floating macrophytes were evaluated based on the superposition of the manually vectored areas and the areas obtained automatically. In addition to the visual assessment, the area automatically mapped and manually obtained for the different macrophyte polygons were compared and the validation metrics were calculated for performance evaluation.

## 4. Results

### 4.1. System Overview

The QDA-System architecture (Figure 3) was defined taking into account the concept of micro services. The application was developed considering small services or independent modules that act together to provide system functionalities, communicating with each other through APIs. The main advantages of this approach are that it is highly scalable and easy to develop in the cloud. From a development point of view, it allows parallel development, making the production process and bug fixing more agile.

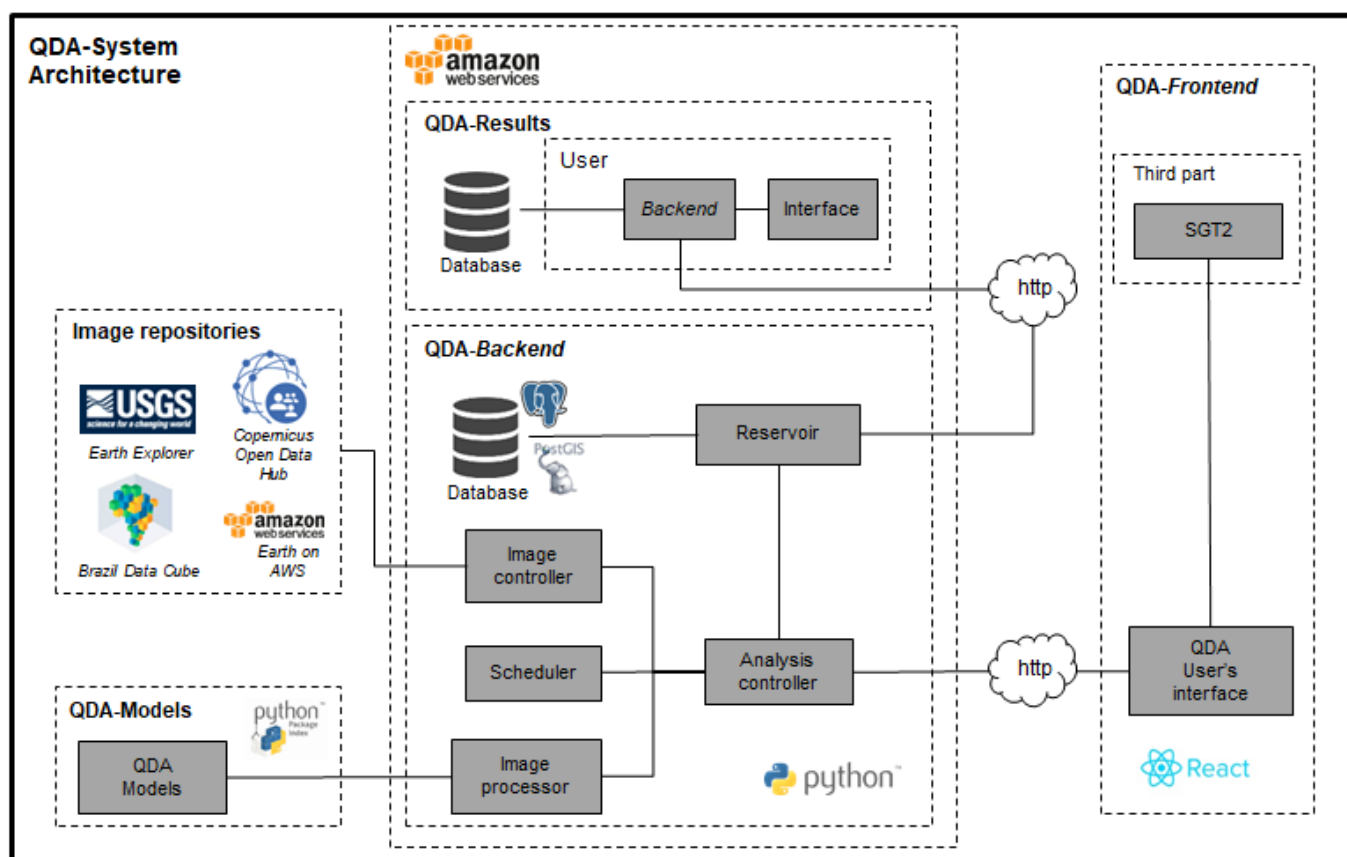


Figure 3. QDA-System architecture.

The architecture of the QDA-System is comprised of substructures each with its respective modules, as described below:

1. QDA-Results: substructure comprised of a backend and a frontend (with Graphics User Interface) so that system users can upload auxiliary data to the system;
2. QDA-Models: this substructure is a module, which has become a public domain project. It has the implementation of bio-optical models found in the literature to assess water quality through the analysis of satellite images. It can be accessed from the Python Package Index (PyPI) package repository <https://pypi.org/project/qda-modelos/> (accessed on 5 January 2022);
3. QDA-Backend: substructure comprised of different modules:
  - Analysis controller: It is activated by the scheduler module and it performs the verification and the obtainment of data present in the reservoir module. It performs the described analysis and it manages the image processing modules;
  - Image processor: It performs the pre-processing of images, uses the module imported from the QDA-Models to estimate the parameters, and it manages the life cycle of an execution;
  - Image controller: It abstracts the image source and it stores and retrieves preprocessed images (if necessary);
  - Reservoirs: This is the module for registering a reservoir;
  - Scheduler: It is responsible for activating the analysis controller module and keeping a schedule of executions.
4. QDA-Frontend: This is a frontend substructure responsible for communicating with the backend and for showing the user a graphical interface based on React technology (<https://reactjs.org/> (accessed on 20 December 2021)). It is user-friendly and it is easy to interpret when checking the data processed by the system.

#### 4.2. System Interface

The pilot version of the QDA-System interface allows the user access to three views of the monitored water body: (1) dashboard view; (2) alerts view; and (3) analysis view.

The dashboard view allows the user to visualize the current information generated using the last image acquired, with the visualization being segmented by the sub-area of the monitored water body. The screen displays the generated alerts, a water quality map, and a table with a summary of monitored parameters and their trends (worsening, stable, or improving). It also shows the date of the last image processed and its percentage of invalid pixels due to the presence of clouds or shadows.

The alerts view allows the user to view and to manage the alerts generated for the parameters of interest. In this view, it is possible to filter alerts by reservoir sub-area, parameter of interest, period or date, and alert status (recognized and unrecognized). Alerts are displayed with their spatial distribution on the reservoir map, and they are also summarized in a list and a table form. The alerts automatically generated by the QDA-System can be recognized by the user.

The analysis view allows the user to access different functionalities such as querying the space–time history of monitored parameters and indices through thematic maps and time series graphs displayed on the screen, viewing additional layers such as in situ sampling points and points with other uses (e.g., recreation, catchment for public water supply, irrigation), and areas covered by floating macrophytes.

#### 4.3. Pilot Application

##### 4.3.1. Model Calibration

The model calibration was considered satisfactory for the nine water quality parameters selected for the pilot application of the QDA-System (Table 2). The models derived directly from satellite images (optically active parameters) showed results that are corroborated by the literature [3], being the models with the best performance for SDD, TSS, and turbidity based on single band relation (red band corrected for sun glint effect). For the Chl-*a* concentration, the model with the best fit was based on a polynomial relation with the Normalized Difference Chlorophyll Index (NDCI) [20]. The  $R^2$  values obtained for optically active parameter models were higher than those reported in the literature [15], highlighting the turbidity model that showed excellent calibration performance ( $R^2 = 0.94$ ).

**Table 2.** Summary of model calibration.

| Parameter     | Unit  | <i>n</i> | $R^2$ | Model with Best Calibration Performance  |
|---------------|-------|----------|-------|--|
| Chl- <i>a</i> | µg/L  | 29       | 0.89  | $Y = 229.95\text{NDCI}^2 + 122.58\text{NDCI} + 19.964$   |
| SDD           | m     | 62       | 0.83  | $Y = 1.407\text{Ln}(B4_{\text{corr}}) - 3.1782$  |
| TSS           | mg/L  | 22       | 0.73  | $Y = 3.9215e^{(66.727B4_{\text{corr}})}$   |
| Turbidity     | NTU   | 62       | 0.94  | $Y = 9459.9B4_{\text{corr}}^2 - 238.53B4_{\text{corr}} + 6.0006$                                 |
| Conductivity  | µS/cm | 48       | 0.46  | $Y = 1.0144\text{SST} + 17.075$  |
| DO            | mg/L  | 30       | 0.50  | $Y = 16.213\left(\frac{1}{\text{SDD}}\right)^2 - 3.669\left(\frac{1}{\text{SDD}}\right) + 6.861$ |
| Nitrate       | mg/L  | 33       | 0.69  | $Y = 0.205\text{Turbidity} + 1.6134$   |
| pH            | -     | 99       | 0.11  | $Y = 0.0073\text{Conductivity} + 6.5858$   |

$B4_{\text{corr}}$  refers to Sentinel-2 B4 images corrected for the sun glint effects. The glint effect was removed by subtracting the values of B11 (short wave infrared) from B4 (red) values [21].

As expected the models derived indirectly from satellite images (optically inactive parameters) showed lower performance than the models derived directly, with  $R^2$  values between 0.11 and 0.69. The best calibration performances were obtained for nitrate ( $R^2 = 0.69$ ) and DO ( $R^2 = 0.50$ ) parameters. The nitrate model was based on a linear relation with SST, whereas the DO model was based on a polynomial relation with the inverse of



SDD. The electric conductivity and pH models showed the poorest performance during the calibration procedure.

For the detection of floating macrophytes, the model with the best performance during the calibration procedure was based on NDAVI using a detection threshold equal to 0 ( $R^2 = 0.99$ ). In this case, NDAVI values higher than zero are considered floating macrophytes whereas values equal to or less than zero are considered water.

#### 4.3.2. Model Validation

Regarding the models obtained directly from satellite images, the results of validation (Table 3) indicate an excellent performance of the adjusted model for the estimation of turbidity, showing a strong agreement between the estimated and observed values ( $R^2 = 0.87$ ), low absolute mean deviation (MAD = 2.87 NTU) and low RMSE (3.05 NTU). The turbidity model adjusted for the FCHR performed better than those presented in other studies (except for the MAPE validation metric), even when compared with more sophisticated models based on neural networks [15].

**Table 3.** Summary of model validation.

| Parameter            | <i>n</i> | $R^2$ | MAD   | MSE    | RMSE  | MAPE   |
|----------------------|----------|-------|-------|--------|-------|--------|
| Floating macrophytes | 18       | 0.99  | -     | -      | 0.77  | 10.13  |
| Chl- <i>a</i>        | 15       | 0.00  | 1.670 | 4.51   | 2.12  | 60.00  |
| SDD                  | 49       | 0.49  | 0.83  | 1.00   | 1.00  | 50.31  |
| TSS                  | 10       | 0.70  | 17.89 | 401.48 | 20.04 | 43.47  |
| Turbidity            | 47       | 0.87  | 2.87  | 9.33   | 3.05  | 125.16 |
| Conductivity         | 20       | 0.11  | 7.52  | 136.70 | 11.69 | 20.51  |
| DO                   | 44       | 0.10  | 0.67  | 1.05   | 1.02  | 9.35   |
| Nitrate              | 14       | 0.51  | 0.253 | 0.095  | 0.307 | 11.64  |
| pH                   | 43       | 0.11  | 0.611 | 0.472  | 0.687 | 7.892  |

The adjusted models for estimation of SDD and TSS showed a low performance compared to the turbidity model, but they were also considered very satisfactory. The model for water transparency presented a MAD of 0.83 m and an RMSE of 1 m, whereas the model for TSS presented a MAD of 17.89 mg/L and an RMSE of 20.04 mg/L.

In turn, for the adjusted model to estimate chlorophyll-*a* concentration, the validation results indicated a weak agreement between the estimated and the observed values ( $R^2 < 0.01$ ). The analysis of the errors obtained with the model adjusted to estimate chlorophyll-*a* concentration showed results considered favorable compared to those presented in the literature [15], with a MAD of 1.84  $\mu\text{g/L}$  and an RMSE of 2.23  $\mu\text{g/L}$ . The historical data from water quality monitoring indicated low concentrations of chlorophyll-*a* in the reservoir, and in 73% of the samples collected between June/2015 and February/2021 the result obtained in the laboratory was less than the quantification limit (1  $\mu\text{g/L}$ ).

For the parameters obtained indirectly from images, the best validation performance was obtained for the nitrate model, with low error metrics (e.g., RMSE = 0.3 mg/L) and moderate agreement between the estimated and the observed values ( $R^2 = 0.51$ ). The DO and pH models also presented low errors but a weak agreement between the estimated and the observed values ( $R^2 = 0.11$ ). Finally, the model to estimate electric conductivity of water exhibited the poorest performance with a MAPE close to 20% and a weak agreement between the estimated and the observed values ( $R^2 = 0.10$ ).

The model adjusted to detect floating macrophytes showed a favorable validation performance, with high agreement between detected and vectorized values ( $R^2 = 0.99$ ) and a MAPE near 10% (0.77 hectares).

### 4.3.3. User’s Interface and Data Access

Figures 4–6 show the three different views developed to access and to query the data through the user’s interface of the QDA-System: (1) dashboard view, (2) alert view and (3) analysis view. The dashboard view developed for the pilot application (Figure 4) shows the actual status of the FCHR water quality based on the last MSI image processed by the system. In this case, the information is presented for three different reservoir sectors predefined for the FCHR: “Barramento,” “Central,” and “Cabeceira”.

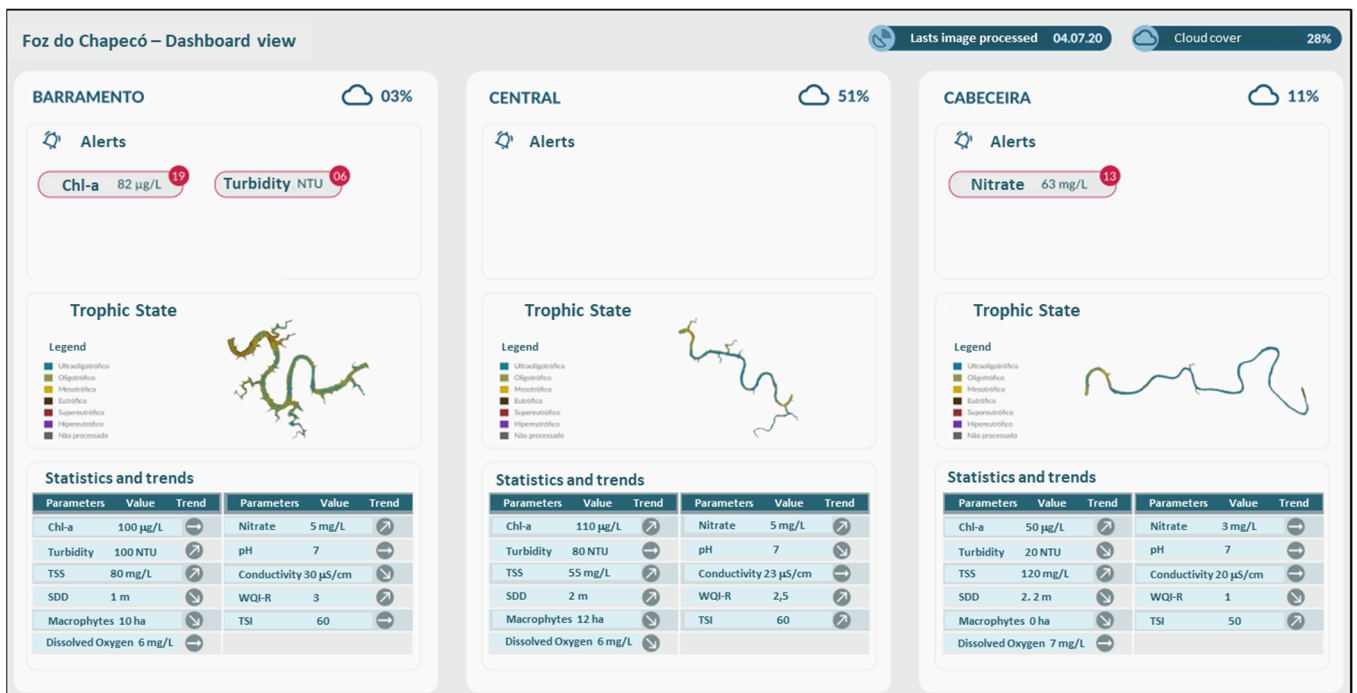


Figure 4. Dashboard view.

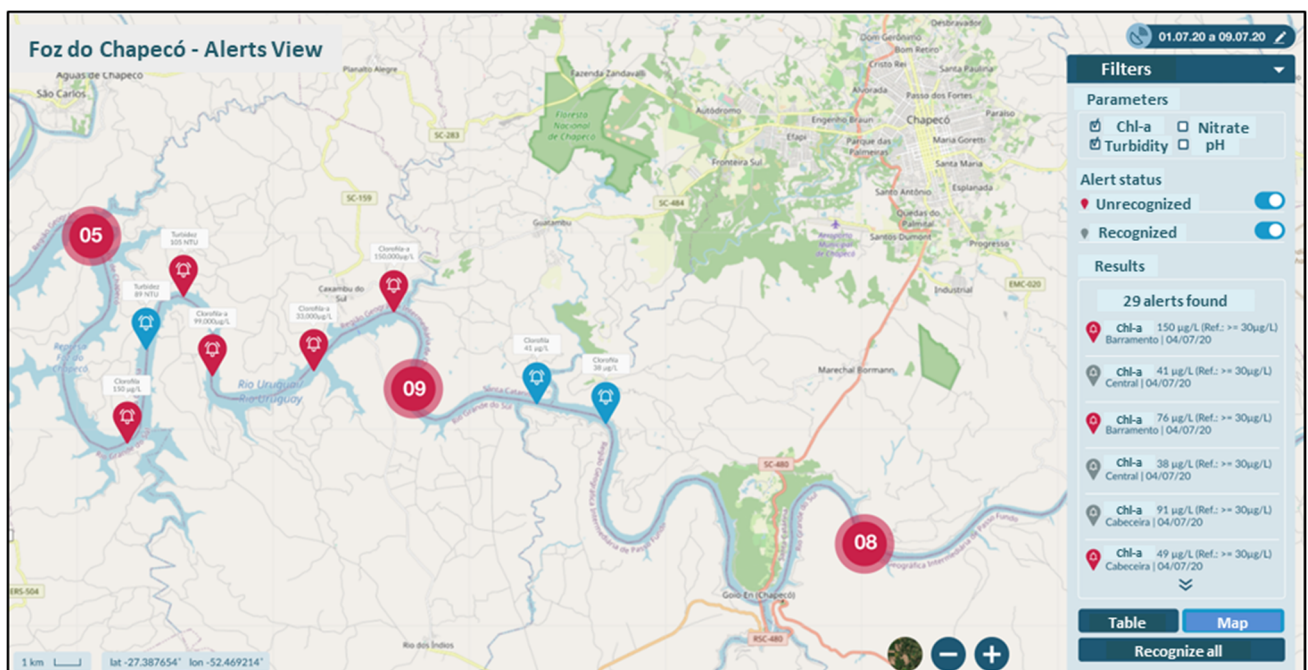


Figure 5. Alerts view.

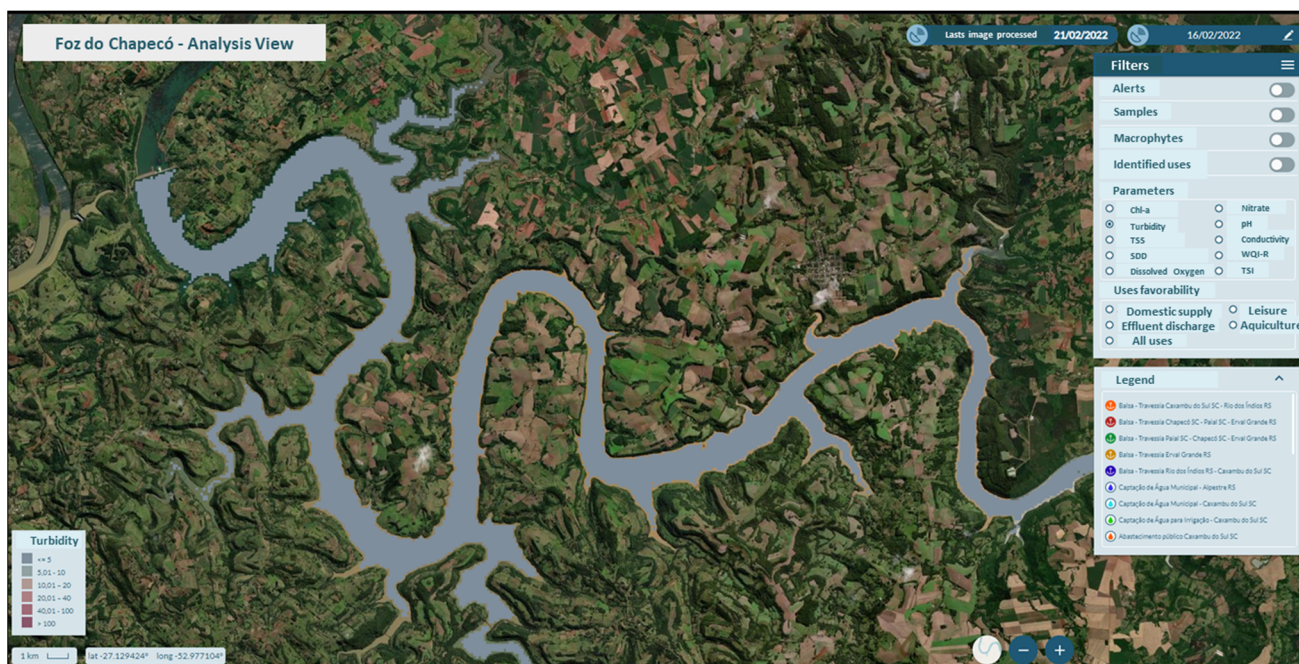


Figure 6. Analysis view.

For the example shown in Figure 4, the “Barramento” sector presented 19 alerts for chlorophyll-*a* concentration and 6 alerts for turbidity, considering the image processed on 4 July 2020. The “Cabeceira” sector presented 13 alerts for turbidity, while in the “Central” sector no alert was generated by the system. The trophic state presented a steep gradient between the river zone (“Cabeceira”) and the dam zone (“Barramento”), with low trophic levels (ultra-oligotrophic) observed in the “Cabeceira” sector and high trophic levels observed in the “Barramento” sector (eutrophic).

The alert view (Figure 5) allows the user to consult and to manages alerts generated by the system. The user can filter alerts based on a single or a range of MSI image dates, the reservoir sector, the parameter of interest, and the alert status (recognized or not recognized). The alerts can be displayed on the map or in a table format using a color code for the recognized alerts (blue) and unrecognized alerts (red). For the pilot application, the alerts are generated for four parameters (chlorophyll-*a*, nitrate, turbidity, and pH) based on the water quality standards established for class two freshwaters according to Brazilian regulations [22]. An example of a query, Figure 5, shows the recognized and the unrecognized alerts which were generated for chlorophyll-*a* and turbidity parameters between 1 July 2020 and 9 July 2020.

Finally, Figure 6 shows the analysis view developed for the pilot application at the FCHR.

Figure 6 shows an example of a query for spatial distribution of turbidity retrieved based on the image acquired on 16 February 2022 for the “Barramento” sector. In this case, turbidity presented a homogeneous pattern with values lower than 5 NTU for the entire sector.

## 5. Conclusions

This paper presents the development and the pilot application of the QDA-System, a cloud-based system to monitor water quality in lakes and reservoirs using remote sensing images. The QDA-System allows the spatial and the temporal monitoring of water quality parameters, emission and management of alerts, and calculation of water quality indexes, such as the trophic state index. The system is an innovative application that combines state of the art remote sensing applied to inland aquatic environments, cloud computing techniques, and software development. Two of the main features of the QDA-System

are its versatility and its scalability, allowing customizations for different areas of interest according to specific monitoring needs and supporting the use of different images (e.g., MSI Sentinel-2 and OLI Landsat-8) and types of models (empirical and semi-empirical).

The pilot application of the QDA-System was implemented to monitor the Foz do Chapecó Hydroelectric Reservoir located in southern Brazil, with the implementation of nine water quality models calibrated and validated specifically for the reservoir. The pilot application is in the initial phase of operation for monitoring the selected reservoir; and, after the testing period, the QDA System will be available to be replicated to other hydroelectric reservoirs, with considerable potential to bring benefits and cost reductions related to water quality monitoring for the entire hydroelectric generation sector in Brazil. In addition, we emphasize that the QDA-System has great potential for application in other areas that also demand routine monitoring of water quality, such as the sanitation sector (public supply reservoirs or monitoring of receiving water bodies) and other industrial applications such as aquaculture.

**Author Contributions:** Data curation, R.Y.; Formal analysis, V.G.; Funding acquisition, M.C.; Investigation, G.S., G.P., J.d.S. and V.G.; Methodology, M.C., E.N. and M.D.; Project administration, M.C.; Software, F.d.S., F.Y., J.d.S., L.S., M.S. and R.Y.; Supervision, E.N., M.S. and M.D.; Validation, G.S., G.P. and M.D.; Visualization, N.B.; Writing—original draft, M.C. All authors have read and agreed to the published version of the manuscript.

**Funding:** This work was supported by Foz do Chapecó Energia S.A. and Energética Barra Grande (BAESA) research and technological development programs through the R&D 00642-2705/2019 project, regulated by Brazilian Electricity Regulatory Agency (ANEEL).

**Informed Consent Statement:** Not applicable.

**Data Availability Statement:** Not applicable.

**Acknowledgments:** We would like to thank the Foz do Chapecó S.A. and the Brazilian Electricity Regulatory Agency (ANEEL) for its encouragement, long-term vision, support, and for believing in the local and national capacity to develop innovative systems with a high degree of technological content. We also thank the Fundação CERTI for creating the necessary conditions for the development of the QDA-System.

**Conflicts of Interest:** The authors declare no conflict of interest.

## References

1. Topp, S.N.; Pavelsky, T.M.; Jensen, D.; Simard, M.; Ross, M.R.V. Research trends in the use of remote sensing for inland water quality science: Moving towards multidisciplinary applications. *Water* **2020**, *12*, 169. [CrossRef]
2. Gholizadeh, M.H.; Melesse, A.M.; Reddi, L. A comprehensive review on water quality parameters estimation using remote sensing techniques. *Sensors* **2016**, *16*, 1298. [CrossRef] [PubMed]
3. Mishra, D.R.; Ogashawara, I.; Gitelson, A.A. *Bio-Optical Modeling and Remote Sensing of Inland Waters*; Elsevier: Amsterdam, The Netherlands, 2017.
4. EOLakeWatch: Satellite Earth Observations for Lake Monitoring. Available online: <https://www.canada.ca/en/environment-climate-change/services/water-overview/satellite-earth-observations-lake-monitoring.html> (accessed on 19 March 2021).
5. U.S. Environmental Protection Agency (EPA). Cyanobacteria Assessment Network (CyAN). Available online: <https://www.epa.gov/water-research/cyanobacteria-assessment-network-cyan> (accessed on 19 March 2021).
6. Morsy, M.M.; Goodal, J.L.; O'Neil, G.L.; Sadles, J.M.; Voce, D.; Hassan, G.; Huxley, C. A cloud-based flood warning system for forecasting impacts to transportation infrastructure systems. *Environ. Model. Softw.* **2018**, *107*, 231–244. [CrossRef]
7. Ferreira, K.R.; Queiroz, G.R.; Câmara, G.; Souza, R.C.M.; Vinhas, L.; Marujo, R.E.O.; Simões, C.A.F.; Noronha, R.; Costa, W.; Arcaño, J.S.; et al. Using remote sensing images and cloud services on aws to improve land use and cover monitoring. In Proceedings of the 2020 IEEE Latin American GRSS & ISPRS Remote Sensing Conference (LAGIRS), Santiago, Chile, 22–26 March 2020; pp. 207–211.
8. Malthus, T.J.; Lehmann, E.; Ho, X.; Botha, E.; Anstee, J. Implementation of a satellite based inland water algal bloom alerting system using analysis ready data. *Remote Sens.* **2019**, *11*, 2954. [CrossRef]
9. The Foz do Chapecó Power Plant. Available online: <http://www.fozdochapeco.com.br/usina/> (accessed on 2 February 2021).
10. Ecosistêmica Meio Ambiente LTDA (Ecosistêmica). *Foz do Chapecó Reservoir Use Plan*; Ecosistêmica: Porto Alegre, Brazil, 2017.
11. Companhia Ambiental do Estado de São Paulo (CETESB). *Guia Nacional de Coleta e Preservação de Amostras: Água, Sedimento, Comunidades Aquáticas e Efluentes Líquidos*; CETESB: São Paulo, Brazil, 2011.

12. American Public Health Association (APHA). *Standard Methods for the Examination of Water and Waste Water American Public Health Association*; APHA: Washington, DC, USA, 2017.
13. U.S. Environmental Protection Agency (EPA). *Method 300.1: Determination of Inorganic Anions in Drinking Water by Ion Chromatography v. 1.0*; EPA: Cincinnati, OH, USA, 1997.
14. Sentinel-2 Mission. Available online: <https://sentinel.esa.int/web/sentinel/missions/sentinel-2> (accessed on 2 March 2021).
15. Sagan, V.; Peterson, K.T.; Maimaitijiang, M.; Sidike, P.; Sloan, J.; Greeling, B.A.; Maalouf, S.; Adams, C. Monitoring inland water quality using remote sensing: Potential and limitations of spectral indices, bio-optical simulations, machine learning, and cloud computing. *Earth-Sci. Rev.* **2020**, *205*, 103–187. [[CrossRef](#)]
16. Tucker, C.J. Red and photographic infrared linear combinations for monitoring vegetation. *Remote Sens. Environ.* **1979**, *8*, 127–150. [[CrossRef](#)]
17. Huete, A. A comparison of vegetation indices over a global set of TM images for EOS-MODIS. *Remote Sens. Environ.* **1997**, *59*, 440–451. [[CrossRef](#)]
18. Villa, P.; Laini, A.; Bresciani, M.; Bolpagni, R. A remote sensing approach to monitor the conservation status of lacustrine *Phragmites australis* beds. *Wetl. Ecol. Manag.* **2013**, *21*, 399–416. [[CrossRef](#)]
19. Villa, P.; Mousivand, A.; Bresciani, M. Aquatic vegetation indices assessment through radiative transfer modeling and linear mixture simulation. *Int. J. Appl. Earth Obs. Geoinf.* **2014**, *30*, 113–127. [[CrossRef](#)]
20. Mishra, S.; Mishra, D.R. Normalized difference chlorophyll index: A novel model for remote estimation of chlorophyll-*a* concentration in turbid productive waters. *Remote Sens. Environ.* **2012**, *117*, 394–406. [[CrossRef](#)]
21. Curtarelli, V.P.; Barbosa, C.C.F.; Maciel, D.A.; Junior, R.F.; Carlos, F.M.; Novo, E.M.L.M.; Curtarelli, M.P.; da Silva, E.F.F. Diffuse Attenuation of Clear Water Tropical Reservoir: A Remote Sensing Semi-Analytical Approach. *Remote Sens.* **2020**, *12*, 2828. [[CrossRef](#)]
22. Conselho Nacional de Meio Ambiente (CONAMA). *Resolução CONAMA n° 357, de 17 de Março de 2005*; CONAMA: Brasília, Brazil, 2005.